

---

# NAS-Bench-360: Benchmarking Diverse Tasks for Neural Architecture Search

---

**Renbo Tu**  
Carnegie Mellon University  
renbo@cmu.edu

**Mikhail Khodak**  
Carnegie Mellon University  
khodak@cmu.edu

**Nicholas Roberts**  
University of Wisconsin-Madison  
nick11roberts@cs.wisc.edu

**Ameet Talwalkar**  
Carnegie Mellon University and Hewlett Packard Enterprise  
talwalkar@cmu.edu

<https://nb360.ml.cmu.edu>

## Abstract

Most existing neural architecture search (NAS) benchmarks and algorithms prioritize performance on well-studied tasks, e.g., image classification on CIFAR and ImageNet. This makes the applicability of NAS approaches in more diverse areas inadequately understood. In this paper, we present **NAS-Bench-360**, a benchmark suite for evaluating state-of-the-art NAS methods for convolutional neural networks (CNNs).<sup>1</sup> To construct it, we curate a collection of ten tasks spanning a diverse array of application domains, dataset sizes, problem dimensionalities, and learning objectives. By carefully selecting tasks that can both interoperate with modern CNN-based search methods but that are also far-afeld from their original development domain, we can use NAS-Bench-360 to investigate the following central question: *do existing state-of-the-art NAS methods perform well on diverse tasks?* Our experiments show that a modern NAS procedure designed for image classification can indeed find good architectures for tasks with other dimensionalities and learning objectives; however, the same method struggles against more task-specific methods and performs catastrophically poorly on classification in non-vision domains. The case for NAS robustness becomes even more dire in a resource-constrained setting, where a recent NAS method provides little-to-no benefit over much simpler baselines. These results demonstrate the need for a benchmark such as NAS-Bench-360 to help develop NAS approaches that work well on a variety of tasks, a crucial component of a truly robust and automated pipeline. We conclude with a demonstration of the kind of future research our suite of tasks will enable. All data and code is made publicly available.

## 1 Introduction

Neural architecture search (NAS) aims to automate the design of deep neural networks, ensuring performance on par with hand-crafted architectures while reducing human labor devoted to tedious architecture tuning (Elsken et al., 2019). With the growing number of application areas of ML, and thus of use-cases for automating it, NAS has experienced an intense amount of study, with significant progress in search space design (Zoph et al., 2018; Liu et al., 2019b; Cai et al., 2019), search efficiency (Pham et al., 2018), and search algorithms (Xu et al., 2020; Li et al., 2021a; White et al., 2021). While the use of NAS techniques may be especially impactful in under-explored or

---

<sup>1</sup>In this work, *NAS method* refers to a combined search space and algorithm pair, not the algorithm alone.

under-resourced domains where less expert help is available, the field has largely been dominated by methods designed for and evaluated on benchmarks in computer vision (Liu et al., 2019b; Ying et al., 2019; Dong & Yang, 2020). There have been a few recent efforts to diversify these benchmarks to settings such as vision-based transfer learning (Duan et al., 2021) and speech and language processing Mehrotra et al. (2021); Klyuchnikov et al. (2020); however, evaluating NAS methods on such well-studied tasks using traditional CNN search spaces does not give a good indication of their utility on more far-afield applications, which have often necessitated the design of custom neural operations (Cohen et al., 2018; Li et al., 2021b).

We make progress towards studying NAS on more diverse tasks by introducing a suite of benchmark datasets drawn from various data domains that we collectively call **NAS-Bench-360**. This benchmark consists of an organized setup of ten suitable datasets that (a) can be evaluated in a unified way using existing NAS approaches and (b) represent diverse application domains, dataset sizes, problem dimensionalities, and learning objectives. We also include standard image classification evaluations as a baseline point of comparison, as many new methods continue to be designed for such tasks.

Following our construction of this suite of tasks, we demonstrate both the usefulness of and need for NAS-Bench-360 by using it to investigate whether modern NAS is useful to practitioners faced with diverse tasks, i.e., whether its success in computer vision is indicative of strong performance on the much broader set of problems to which NAS can conceivably be applied. To address this question, we start with the fact that a common first approach when applying deep learning to a new domain is to try an off-the-shelf CNN; in our case, this will be the Wide ResNet (WRN) (Zagoruyko & Komodakis, 2016). We then consider the scenario of two practitioners: one with only the resources to train one WRN using the default settings and another that has enough to tune WRN using an off-the-shelf hyperparameter optimizer (Li et al., 2018). Both are faced with a decision: *should they use these fixed-architecture baselines or try out the best NAS has to offer?*

Overall, our empirical investigation suggests the following:

1. The less-constrained practitioner might usually do better using NAS—20% relative improvement over WRN on the median task—but risks catastrophic results on specific non-vision applications.
2. The robustness of NAS in the constrained case may be worse: the practitioner is likely better-off simply using the simple off-the-shelf WRN, as its median rank across NAS-Bench-360’s ten tasks is the same as that of our candidate NAS method.

These results are obtained via experiments using two well-studied modern search spaces: the cell-based DARTS space (Liu et al., 2019b) and the efficiency-focused DenseNAS space (Fang et al., 2020). Each space is paired with a search method known to find well-performing architectures on ImageNet, specifically the state-of-the-art GAEA PC-DARTS (Li et al., 2021a) for the former and the original weight-sharing algorithm used by DenseNAS for the latter. Note that our assessment includes a more holistic comparison using performance profiles (c.f. Figure 1) to reinforce these ranking-based comparisons, which are useful but can miss a lack of robustness or exaggerate minor differences between methods.

The initial experimental results enabled by NAS-Bench-360 suggest that the robustness of modern search methods to diverse tasks beyond image classification is mixed at best. At the same time, our set of tasks can serve as a crucial tool for investigating and rectifying this issue, and it is thus important for moving towards a truly automated pipeline containing NAS. In particular, NAS-Bench-360 will facilitate such progress via a diverse array of tasks for validating NAS methods that are not only challenging, real-life problem settings but also computationally accessible for academic researchers with limited budgets. We demonstrate this potential via further studies on the comparative importance of search spaces v. search algorithms and the usefulness of more-customized approaches, specifically by studying a random search (RS) baseline over the DenseNAS space as well as two domain-specific methods: Auto-DeepLab (Auto-DL)(Liu et al., 2019a) for dense prediction and AMBER (Zhang et al., 2021b) for prediction from 1D data. Among other insights, these experiments provide evidence that a more robust NAS may require better search spaces with a wider variety of operations.

The associated datasets and experiment code will remain open-source and accessible at <https://github.com/rtu715/NAS-Bench-360>. Reproducibility of all experiments is assured from open-sourcing all relevant code for the end-to-end procedure, with Docker containers and random seeds provided.

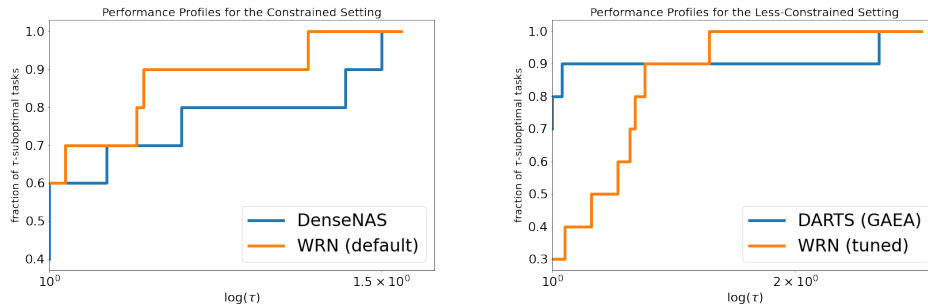


Figure 1: Performance profiles for two settings on all ten tasks in NAS-Bench-360. A larger value indicates a larger fraction of tasks on which the method is within a multiplicative factor  $\tau$  of the best.

## 2 Related Work

Benchmarks have been critical to the development of NAS in recent years. This includes standard evaluation datasets and protocols, of which the most popular are the CIFAR-10 and ImageNet routines used by DARTS (Liu et al., 2019b). Another important type of benchmark has been tabular benchmarks such as NAS-Bench-101 (Ying et al., 2019), NAS-Bench-201 (Dong & Yang, 2020), and NAS-Bench-1Shot1 (Zela et al., 2020); these benchmarks exhaustively evaluate all architectures in their search spaces, which is made computationally feasible by defining simple searched cells. Consequently, they are less expressive than the DARTS cell (Liu et al., 2019b), often regarded as the most powerful search space in the cell-based regime. Notably, our benchmark is *not* a tabular benchmark, i.e., we do *not* evaluate every architecture from a fixed search space; instead, the focus is on the organization of a suite of tasks for assessing both NAS algorithms and search spaces, which would necessarily be restricted by fixing a search space for a tabular benchmark. Pre-computing on an expansive search space such as DARTS, with  $10^{18}$  possible architectures, is computationally intractable. Architectures found on lesser search spaces are most likely suboptimal: the vanilla WRN outperforms all networks in the NAS-Bench-201 search space on CIFAR-100.

While NAS methods and benchmarks have generally been focused on computer vision, recent work such as AutoML-Zero (Real et al., 2020) and XD-operations (Roberts et al., 2021) has started moving towards a more generically applicable set of tools for AutoML. However, even more recent benchmarks that do go beyond the most popular vision datasets have continued to focus on well-studied tasks, including vision-based transfer learning (Duan et al., 2021), speech recognition (Mehrotra et al., 2021), and natural language processing (Klyuchnikov et al., 2020). We aim to go beyond such areas to evaluate the potential of NAS to automate the application of ML in truly under-explored domains. One analogous work to ours in the field of meta-learning is the Meta-Dataset benchmark of few-shot tasks (Triantafillou et al., 2020), which similarly aimed to establish a wide-ranging set of evaluations for that field. For our inclusion of diverse tasks, we title our benchmark NAS-Bench-360 to resemble the idea of a 360-degree camera that covers all possible directions.

## 3 NAS-Bench-360: A Suite of Diverse and Practical Tasks

In this section, we introduce the NAS setting targeted by our benchmark, our motivation for organizing a new set of diverse tasks as a NAS evaluation suite, and our task-selection methodology. We report evaluations of specific algorithms on this new benchmark in the next section.

### 3.1 Neural Architecture Search: Problem Formulation and Baselines

For completeness and clarity, we first formally discuss the architecture search problem itself, starting with the extended hypothesis class formulation Li et al. (2021a). Here the goal is to use a dataset of points  $x \in \mathcal{X}$  to find parameters  $\mathbf{w} \in \mathcal{W}$  and  $a \in \mathcal{A}$  of a parameterized function  $f_{\mathbf{w},a} : \mathcal{X} \mapsto \mathbb{R}_{\geq 0}$  that minimize the expectation  $\mathbb{E}_{x \sim \mathcal{D}} f_{\mathbf{w},a}(x)$  for some test distribution  $\mathcal{D}$  over  $\mathcal{X}$ ; here  $\mathcal{X}$  is the input space,  $\mathcal{W}$  is the space of model weights, and  $\mathcal{A}$  is the set of architectures. For generality, we do not require the training points to be drawn from  $\mathcal{D}$  to allow for domain adaptation, as is the case for one

of our tasks, and we do not require the loss to be supervised. Note also that the goal here does not depend on computational or memory efficiency, which we do not focus on in our evaluations; our restriction is only that the entire pipeline can be run on an NVIDIA V100 GPU.

Notably, this formulation makes no distinction between the model weights  $\mathbf{w}$  and architectures  $a$ , treating both as parameters of a larger model. Indeed, the goal of NAS may be seen as similar to model design, except now we include the design of an (often-discrete) *architecture space*  $\mathcal{A}$  such that it is easy to find an architecture  $a \in \mathcal{A}$  and model weights  $\mathbf{w} \in \mathcal{W}$  whose test loss  $\mathbb{E}_{\mathcal{D}} f_{\mathbf{w},a}$  is low using a search algorithm. This can be done in a one-shot manner—simultaneously optimizing  $a$  and  $\mathbf{w}$ —or using the standard approach of first finding an architecture  $a$  and then keeping it fixed while training model weights  $\mathbf{w}$  using a pre-specified algorithm such as stochastic gradient descent (SGD).

This formulation also includes non-NAS methods by allowing the architecture search space to be a singleton. When the sole architecture is a standard and common network such as WRN (Zagoruyko & Komodakis, 2016), this yields a natural baseline with an algorithm searching for training hyperparameters, not architectures. On the other hand, any architecture space  $\mathcal{A}$  allows for non-one-shot methods to search for architectures, such as random search through repeatedly sampling architectures and evaluating them from partial training. We adopt this simple method as our random baseline. For our empirical investigation, we compare the performance of state-of-the-art NAS approaches against that of the two baselines.

### 3.2 Task Selection: Motivation and Methodology

Curating a diverse, practical set of tasks for the study of NAS is our primary motivation behind this work. We observe that past NAS benchmarks focused on creating larger search spaces and more sophisticated search methods for neural networks. However, the utility of these search spaces and methods are only evaluated on canonical computer vision datasets. On a broader range of problems, whether these new methods can improve upon simple baselines remains an open question. This calls for the introduction of new datasets lest NAS research overfits to the biases of CIFAR-10 and ImageNet. By identifying these possible biases, future directions in NAS research can be better primed to suit the needs of practitioners and to increase the deployment of NAS.

Summarized in Table 1, NAS-Bench-360 is comprised of problems that are conducive to processing by convolutional neural networks, which includes a trove of applications associated with spatial and temporal data, spanning single and multiple dimensions. Most current NAS methods are not implemented to search for other types of architectures to process tabular data and graph data. Therefore, we have set this scope for our investigation. During the selection of tasks, diversity is our primary consideration. We define the following axes of diversity to govern our task-filtering process: the first is problem dimensionality, including both 2D with matrix inputs and 1D with sequence inputs; the second is dataset size, for which our selection spans the scale from 1,000 to 1,000,000; the third is problem type, divisible into tasks requiring a singular prediction (point prediction) and multiple predictions (dense prediction); fourth and finally, diversity is achieved through selecting tasks from various learning objectives from applications of deep learning, where introducing NAS could improve upon the performance of handcrafted neural networks.

In lieu of providing raw data, we perform data pre-processing locally and store the processed data on a public Amazon Web Service’s S3 data bucket with download links available on our website. Our data treatment largely follows the procedure defined by the researchers who provided them. This enhances reproducibility by ensuring the uniformity of input data for different pipelines. Specific pre-processing and augmentation steps are described below.

**CIFAR-100: Standard image classification** As a starting point of comparison to existing benchmarks, we include the **CIFAR-100** task (Krizhevsky, 2009), which contains RGB images from natural settings to be classified into 100 fine-grained categories. CIFAR-100 is preferred over CIFAR-10 because it is more challenging and suffers less from over-fitting in previous research.

**Spherical: Classifying spherically projected CIFAR-100 images** To test NAS methods applied to natural-image-like data, we consider the task of classifying spherical projections of the CIFAR-100 images, which we call **Spherical**. In addition to scientific interest, spherical image data is also present in various applications, such as omnidirectional vision in robotics and weather modeling in meteorology, as sensors usually produce distorted image signals in real-life settings. To create

Table 1: Information of tasks in NAS-Bench-360

Task name	Size	Dim.	Type	Learning objective	New to NAS
CIFAR-100	60K	2D	Point	Classify natural images into 100 classes	
Spherical	60K	2D	Point	Classify spherically projected images into 100 classes	✓
NinaPro	3956	2D	Point	Classify sEMG signals into 18 classes corresponding to hand gestures	✓
FSD50K	51K	2D	Point (multi-label)	Classify sound events in log-mel spectrograms with 200 labels	✓
Darcy Flow	1100	2D	Dense	Predict the final state of a fluid from its initial conditions	✓
PSICOV	3606	2D	Dense	Predict pairwise distances between residuals from 2D protein sequence features	✓
Cosmic	5250	2D	Dense	Predict propablistic maps to identify cosmic rays in telescope images	✓
ECG	330K	1D	Point	Detecting atrial cardiac disease from a ECG recording via classification	✓
Satellite	1M	1D	Point	Classify satellite image pixels' time series into 24 land cover types	✓
DeepSEA	250K	1D	Point (multi-label)	Predicting chromatin states and binding states of RNA-binding sequences	

Spherical CIFAR, we project the planar signals of the CIFAR images to the northern hemisphere and add a random rotation to produce spherical signals for each channel following the procedure specified in Cohen et al. (2018). The resulting images are  $60 \times 60$  pixels with RGB channels.

**NinaPro: Classifying electromyography signals** **NinaPro** moves away from the image domain to classify hand gestures indicated by electromyography signals. For this, we use a subset of the NinaPro DB5 dataset (Atzori et al., 2012) in which two Myo armbands collect EMG signals from 10 test individuals who hold 18 different hand gestures to be classified. These armbands leverage data from muscle movement, which is collected using electrodes in the form of wave signals. Each wave signal is then sampled using a wavelength and frequency prescribed in Côté-Allard et al. (2019) to produce 2D signals.

**FSD50K: Labeling sound events** **FSD50K** (Fonseca et al., 2020) is derived from the larger Freesound dataset (Fonseca et al., 2017) of Youtube videos with 51,000 clips totaling more than 100 hours of sound. These clips are manually labeled and equally distributed in 200 classes from the AudioSet ontology (Gemmeke et al., 2017). Each clip could receive multiple labels. Unlike TIMIT (Garofolo, 1993), FSD50K does not focus exclusively on sounds of spoken language but includes sound events from physical sources and production mechanisms. The mean average precision (mAP) is used to evaluate classification results.

**Darcy Flow: Solving partial differential equations (PDEs)** Our first regression task, **Darcy Flow**, focuses on learning a map from the initial conditions of a PDE to the solution at a later timestep. This application aims to replace traditional solvers with learned neural networks, which can output a result in a single forward pass. The input is a 2d grid specifying the initial conditions of a fluid, and the output is a 2d grid specifying the fluid state at a later time, with the ground truth being the result computed by a traditional solver. We report the mean square error (MSE or  $\ell_2$ ).

**PSICOV: Protein distance prediction** **PSICOV** studies the use of neural networks in the protein folding prediction pipeline, which has recently received significant attention to the success of methods like AlphaFold (Jumper et al., 2020). While the dataset and method they use are too large-scale for our purposes, we consider a smaller set of protein structures to tackle the specific problem of inter-residual distance predictions outlined in Adhikari (2020b). 2D large-scale features are extracted from protein

sequences, resulting in input feature maps with a massive number of channels. Correspondingly, the labels are pairwise-distance matrices with the same spatial dimension. The evaluation metric is mean absolute error (MAE or  $\ell_1$ ) computed on distances below  $8 \text{ \AA}$ , referred to as  $\text{MAE}_8$ .

**Cosmic: Identifying cosmic ray contamination** Images from space-based facilities are prone to corruption by charged particles collectively referred to as "cosmic rays." Cosmic rays on images should be identified and masked before the images are used for further analysis (Zhang & Bloom, 2020). The **Cosmic** task uses imaging data of local resolved galaxies collected from the Hubble Space Telescope. Inputs and outputs are same-size 2D matrices, with the output predicting whether each pixel in the input is an artifact of cosmic rays. We report the false-negative rate (FNR) of identification results.

**ECG: Detecting heart disease** Electrocardiograms are frequently used in medicine to diagnose sinus rhythm irregularities. The **ECG** task is based on the 2017 PhysioNet Challenge (Clifford et al., 2017), with 9 to 60-second ECG recordings sampled at 300 Hz and labeled using four classes: normal, disease, other, or noisy rhythms. Recordings are processed using a fixed sliding window of 1,000 ms and stride of 500 ms. We report the F1-score according to the challenge’s guidelines.

**Satellite: Satellite image time series analysis** Satellite image time series (SITS) are becoming more widely available in earth monitoring applications. Our dataset comes from Formosat-2 satellite images acquired over Toulouse, France (Petitjean et al., 2012). Available in multiple channels, SITS track the land cover changes over several years as each pixel in the image represents a geographical region. The goal of the **Satellite** task is to generate land cover maps for geo-surveying. Specifically, a series of pixels in a given color channel constitute a time series to be classified into 46 land cover types.

**DeepSEA: Predicting functional effects from genetic sequences** Predicting chromatin effects of genetic sequence alterations is a significant challenge in the field to understand genetic diseases. **DeepSEA** (Zhou & Troyanskaya, 2015), provides a compendium of genomic profiles from the Encyclopedia of DNA Elements (ENCODE) project (Consortium et al., 2004) to train a predictive model estimating the behavior of chromatin proteins, divided into 919 categories. Due to computation constraints, we subsample 36 of these categories as per Zhang et al. (2021a) and further take 5% of the training data for prediction. We report the area under the receiver operating characteristic (AUROC) following the previous work.

## 4 Experimental design

Having detailed our construction of NAS-Bench-360, we now describe a set of experiments to demonstrate its usefulness for evaluating NAS methods and guiding research on diverse tasks. In this section, we first specify the different NAS methods and baselines we compare, followed by the experimental and reproducibility setup we follow. The resulting evaluations are reported in Table 2, aggregate performance in Table 3, and performance profiles in Figure 2.

### 4.1 Baselines and Search Procedures

As noted in Section 1, our initial experiments focus on two practitioners with different resource settings, one with enough compute to tune a WRN and another who can only train it once with the default hyperparameters. In matching these settings, we focus on two well-known search paradigms: cell-based NAS (using DARTS (Liu et al., 2019b)) and macro NAS (using DenseNAS (Fang et al., 2020)). We further compare these approaches to two customized NAS methods: Auto-DeepLab (Liu et al., 2019a) for 2D dense prediction and AMBER (Zhang et al., 2021b) for 1D prediction. We detail these approaches below.

**Wide ResNet with Hyperparameter Tuning** Architectures based on ResNet He et al. (2016) are a common first choice by practitioners faced with a new domain (Fonseca et al., 2020; Adhikari, 2020b); it is thus a natural source of fixed-architecture baselines for our study. We use the Wide ResNet variant (Zagoruyko & Komodakis, 2016) with 16 layers and a widen factor of 4, and apply its original training routine directly for the constrained practitioner. For the other practitioner, we wrap

Table 2: Performance of NAS and the WRN baselines across the tasks of NAS-Bench-360. Methods are divided into efficient methods (DenseNAS and fixed WRN) that take 1-10 GPU-hours, more expensive methods (DARTS and WRN tuned by ASHA) that take 10-100+ GPU-hours, and specialized methods (Auto-DL and AMBER). All results are averages of three random seeds.

Search space	Search algorithm	CIFAR-100 0-1 error <sup>l</sup>	Spherical 0-1 error <sup>l</sup>	Darcy Flow relative $\ell_2$ <sup>l</sup>	PSICOV MAE <sub>8</sub> <sup>l</sup>	Cosmic FNR <sup>l</sup>
WRN	default	23.35±0.05	85.77±0.71	0.073±0.001	3.84±0.053	51.76±2.09
DenseNAS	random	25.49±0.41	71.23±1.65	0.071±0.006	3.70±0.06	70.42±6.07
DenseNAS	original	25.98±0.38	72.99±0.95	0.10±0.01	3.84±0.15	79.52±2.20
WRN	ASHA	23.39±0.01	75.46±0.40	0.066±0.00	3.84±0.05	37.53±10.16
DARTS	GAEA	24.02±1.92	48.23±2.87	0.026±0.001	2.94±0.13	31.15±3.48
Auto-DL	DARTS	n/a	n/a	0.049±0.005	6.73±0.73	99.79±0.02
Search space	Search algorithm	NinaPro 0-1 error <sup>l</sup>	FSD50K mAP <sup>h</sup>	ECG F1 score <sup>h</sup>	Satellite 0-1 error <sup>l</sup>	DeepSEA AUROC <sup>h</sup>
WRN	default	6.78±0.26	0.08±0.001	0.57±0.01	15.49±0.03	0.60±0.001
DenseNAS	random	8.45±0.56	0.40±0.001	0.58±0.01	13.91±0.13	0.60±0.001
DenseNAS	original	10.17±1.31	0.36±0.002	0.60±0.01	13.81±0.69	0.60±0.001
WRN	ASHA	7.34±0.76	0.09±0.03	0.57±0.01	15.84±0.52	0.59±0.002
DARTS	GAEA	17.67±1.39	0.06±0.02	0.66±0.01	12.51±0.24	0.64±0.02
AMBER	ENAS	n/a	n/a	0.67±0.015	12.97±0.07	0.68±0.01

<sup>h/l</sup> a higher / lower value of the metric indicates better performance.

the training procedure with a hyperparameter tuner, ASHA (Li et al., 2018), an asynchronous version of Hyperband (Li et al., 2017). Given a range for each hyperparameter, ASHA uniformly samples configurations and uses brackets of elimination: at each round, each configuration is trained for some epochs, before the algorithm selects the best-performing portion based on validation metrics. This procedure is useful for finding suitable hyperparameters in an easy-to-use, automated fashion.

**Cell-based Search Using DARTS** The first NAS paradigm we consider is cell-based NAS. These methods first search for a genotype, a cell containing neural operations. During evaluation, an architecture is constructed by replicating the searched cell and stacking them together. The most popular search space for this approach is DARTS (Liu et al., 2019b), which assigns one of eight operations to six edges in two types of cells: “normal” cells preserve the shape of the input while “reduction” cells downsample it. For dense tasks, we do not use the reduction cell to prevent introducing a bottleneck. For 1D tasks, all convolutions in the cell are converted from 2D to 1D. Finally, to adhere to standard ML practices, we do *not* adapt the standard DARTS pipeline from the original paper. As this search space has been heavily studied, we use as a search routine a recent approach, GAEA PC-DARTS (GAEA), that achieves some of the best-known results on CIFAR-10 and ImageNet (Li et al., 2021a). This NAS approach, due to its heavy retraining routine, is compared to the tuned WRN baseline of the less-resource-constrained practitioner.

**Macro NAS Using DenseNAS** The second NAS paradigm we consider is macro NAS. Instead of building from a fixed cell, it requires the specification of a supernet with different inter-connected blocks. These blocks and connections are then pruned to construct an architecture. For our benchmark, we choose a recent search space, DenseNAS (Fang et al., 2020), which has near state-of-the-art results on ImageNet. DenseNAS searches for architectures with densely-connected, customizable routing blocks to emulate DenseNet (Huang et al., 2017). In our experiments, we use the ResNet-based search space, DenseNAS-R1, which contains all neural operations of the WRN backbone. For 2D tasks, we adapt two super networks from the one used for ImageNet as inputs to the search algorithm. The super network for dense tasks maintains the same spatial dimensions without downsampling to avoid bottlenecks, and we lower the learning rate for evaluating architectures to prevent divergence. For transferring to 1D tasks, all network operations are switched from 2D to 1D. Other training and evaluation procedures are identical to those in the original paper and uniform across all tasks. DenseNAS is quick to search and evaluate, making it comparable to the fixed WRN baseline.

Table 3: Median rank and performance improvement over WRN across NAS-Bench-360.

Search space Search algorithm	WRN default	DenseNAS original	DenseNAS random	WRN ASHA	DARTS GAEA	Auto-DL DARTS	AMBER ENAS
Median rank	4.0	4.0	4.0	3.5	1.5	6.0 <sup>†</sup>	1.0 <sup>†</sup>
% better than WRN*	0.0%	2.53%	0.0%	0.0%	20.1%	-75.3% <sup>†</sup>	20.0% <sup>†</sup>

\* relative improvement over the default (untuned) WRN baseline

<sup>†</sup> metric computed only on the subset of three tasks on which the method was evaluated

We apply another search method to the fixed DenseNAS space to study the relative importance of search algorithms. Random search is implemented through randomly sampling architectures from the DenseNAS space and validating them after a brief training period of 10 epochs before evaluating the best performer. To ensure fairness of comparison, we allot equal GPU hours to random search and regular DenseNAS search, additionally applying a soft constraint that random architecture model sizes should not surpass DenseNAS searched architecture sizes significantly.

**Domain-specific NAS Baselines: Auto-DL and AMBER** To study the importance of search spaces, we further handpick two domain-specific NAS approaches applicable only to a subset of the tasks. Using an encoder-decoder architecture, Auto-DeepLab (Auto-DL) (Liu et al., 2019a) is designed for dense prediction, e.g., semantic segmentation. While the decoder is fixed, Auto-DL searches for an encoder via first-order DARTS. We evaluate Auto-DL on Darcy Flow, PSICOV, and Cosmic tasks.

AMBER (Zhang et al., 2021b) aims to automate neural network design for 1D genomic data. This framework establishes a 12-layer network backbone and parametrizes a long-short term memory network (LSTM) as a controller to search for suitable 1D operations and residual connections, following the ENAS (Pham et al., 2018) optimization protocol. At each step, the controller samples architectures to compute reward based on area under the receiver operating characteristics (AUROC) before outputting the highest-reward architecture. We evaluate AMBER on the ECG, Satellite, and DeepSEA tasks.

## 4.2 Experimental Setup

Below we discuss the main reporting details of our empirical evaluation.

- **Hyperparameter tuning:** As detailed in the Appendix, we use the same hyperparameter ranges across all tasks to tune WRN. The tuning budget is selected to match that of DARTS (GAEA).
- **Aggregation Metrics:** Table 3 contains the median rank and relative improvement over WRN of each method for direct comparison via a single number. We also employ performance profiles (Dolan & Moré, 2002) in Figure 2, an approach that allows an analysis taking into account outliers while not allowing small differences in performance to dominate; as described in Figure 1 these curves denote for each  $\tau$  the fraction of tasks on which a method is no worse than a  $\tau$ -factor from the optimal.
- **Software and hardware:** We adopt the free, open-source software *Determined*<sup>2</sup> for experiment management, hyperparameter tuning, and cloud deployment. All experiments are performed on a single p3.2xlarge instance with an NVIDIA V100 GPU. Costs in GPU-hours are in the appendix.

## 5 Discussion

We conclude our presentation of NAS-Bench-360 via an analysis that (a) reveals new insights about the capabilities and robustness of current NAS methods and (b) demonstrates how our benchmark can enable critical next steps in NAS research. In particular, we start by considering our two practitioners faced with a choice of spending their limited compute on a (possibly tuned) fixed-architecture CNN or trying to find a better architecture using NAS. With this study, we investigate whether modern NAS methods perform well beyond the tasks for which they were designed.

1. A surface-level analysis suggests that under light resource constraints, modern NAS in the form of DARTS (GAEA) is quite robust to a wide variety of tasks: Table 3 shows it is the highest-

<sup>2</sup>GitHub repository: <https://github.com/determined-ai/determined>



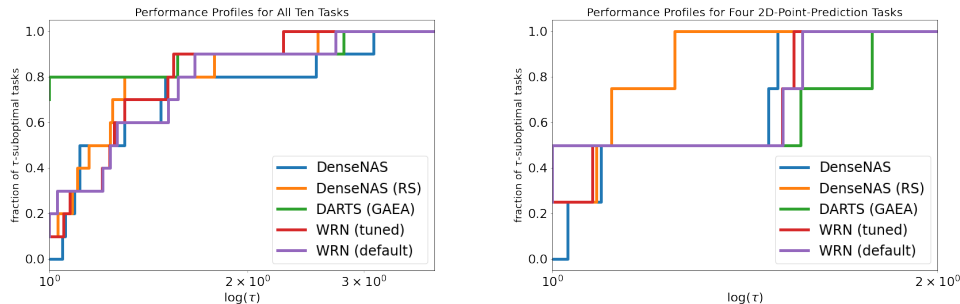


Figure 2: Performance profiles on all tasks (left) and 2D point tasks (right). A larger value indicates a larger fraction of tasks on which the method is within a multiplicative factor  $\tau$  of the best method.

ranked domain-independent method and attains the most significant improvement over the fixed WRN baseline. The performance profile in Figure 2 (left) also seems favorable, although it is overtaken by tuned WRN at a higher  $\tau$ -suboptimality. However, a closer look at 2D point tasks in Figure 2 (right) reveals that DARTS is quite poor there, despite its design domain being image classification; in particular, it performs very poorly on NinaPro and FSD50K. Furthermore, on tasks where it performs well, it can still lag behind expert architectures; for example, on Darcy Flow, networks that use FNO (Li et al., 2021b) or XD (Roberts et al., 2021) operations do much better. Overall, our results suggest that this practitioner can apply NAS and expect to see some improvement, but also risks catastrophically poor performance (e.g., FSD50K) or not getting truly state-of-the-art results (e.g., Darcy Flow).

- Under stronger budget constraints, our experiments strongly suggest that a practitioner should simply apply the default WRN to their problem rather than undergo the additional complexity of using DenseNAS, as the latter attains little-to-no improvement over the former in Table 3 and has a usually-worse performance profiles Figure 2. One bright point, however, is the strong performance of DenseNAS on FSD50K, where it outperforms all methods even while DARTS (GAEA) fails.

These first experiments suggest that the modern NAS methods are not always robust to diverse tasks, especially under resource-constrained settings. We believe that NAS-Bench-360’s main roles as a future benchmark include developing an understanding of the multi-domain performance of existing approaches and guiding research into better NAS methods. While the latter is beyond the scope of this paper, our additional experiments demonstrate how NAS-Bench-360 facilitates the former.

Notably, several results address the question of the relative importance of search space v. search algorithm. For example, Table 3 shows that on DenseNAS, random search is nearly identical to the more sophisticated weight-sharing scheme of the original paper; the two algorithms’ performance profiles are also difficult to distinguish in Figure 2. Furthermore, AMBER—a 1D NAS method whose search space includes larger-kernel convolutions for handling such tasks—does better than GAEA even though it uses an older search algorithm (ENAS). These both suggest that search space design, including the use of a wider variety of operations, may be at least as crucial for success as the search algorithm. This point is reinforced by example tasks such as Darcy Flow, where architectures with more exotic operations substantially outperform our best results, as discussed earlier.

NAS-Bench-360 also reveals failure points of several methods, not just general ones that usually perform quite well such as DARTS (GAEA) but also the objective-specific approach Auto-DL, which despite being designed for dense prediction tasks, does poorly on all those considered here. Understanding when and why these performance drops happen is critical to developing a more robust NAS that is useful not just on average but in more challenging settings.

## 6 Conclusion

NAS-Bench-360 is a new benchmark consisting of ten diverse tasks derived from various fields of research and practice. It is designed for reproducible research on an academic budget that will guide the development of NAS methods and other automated approaches towards more robust

performance across different domains. In initial results, we have demonstrated both the need for such a benchmark and the utility of NAS-Bench-360 specifically for developing new search spaces and algorithms; we welcome researchers to use its tasks to develop new procedures for automating ML.

## 7 Ethics Statement

Within our array of tasks, only NinaPro, ECG, and DeepSEA contain human-derived data. Our chosen subset of NinaPro contains only muscle movement data without any exposure of personal information. The original experiments to acquire NinaPro data are approved by the ethics commission of the canton of Valais, Switzerland (Atzori et al., 2012). The ECG data derives from an open challenge and is provided by the medical device company AliveCor, under the GPL license allowing it for public use. The DeepSEA data derived from ENCODE is part of an international collaborative effort, which is overseen and funded by the National Human Genome Research Institute (NHGRI). For other datasets, we have listed the data licenses in the appendix. While we do not view the specific datasets in NAS-Bench-360 as potential candidates for misuse, the broader goal of applying NAS to new domains comes with inherent risks that may require mitigation on an application-by-application basis.

## 8 Reproducibility Statement

The following measures are taken to ensure reproducibility:

1. We store the processed data in AWS S3, and data splits are the same for all experiments.
2. Code is always executed in a fixed Docker container using a pre-built image on Docker Hub. This guarantees a uniform execution environment and saves users from configuring dependencies.
3. Via the specification of a random seed, *Determined* controls several essential sources of randomness during execution, including hyperparameter sampling and training data shuffling.
4. During training, we validate on the entire validation set, not on a mini-batch, to limit stochasticity.
5. Code and download links of all datasets are available at the repository: <https://github.com/rtu715/NAS-Bench-360>

## Acknowledgements

We thank Maria-Florina Balcan for providing useful feedback. We also thank the Determined AI open-source community for its support. This work was supported in part by DARPA FA875017C0141, the National Science Foundation grants IIS1705121, IIS1838017, IIS2046613 and IIS-2112471, an Amazon Web Services Award, a Facebook Faculty Research Award, funding from Booz Allen Hamilton Inc., a Block Center Grant, a Two Sigma Fellowship Award, and a Facebook Fellowship Award. Any opinions, findings and conclusions or recommendations expressed in this material are those of the author(s) and do not necessarily reflect the views of any of these funding agencies.

## References

- Badri Adhikari. Deepcon: protein contact prediction using dilated convolutional neural networks with dropout. *Bioinformatics*, 36(2):470–477, 2020a.
- Badri Adhikari. A fully open-source framework for deep learning protein real-valued distances. *Scientific reports*, 10(1):1–10, 2020b.
- Manfredo Atzori, Arjan Gijsberts, Simone Heynen, Anne-Gabrielle Mittaz Hager, Olivier Deriaz, Patrick Van Der Smagt, Claudio Castellini, Barbara Caputo, and Henning Müller. Building the ninapro database: A resource for the biorobotics community. In *2012 4th IEEE RAS & EMBS International Conference on Biomedical Robotics and Biomechatronics (BioRob)*, pp. 1258–1265. IEEE, 2012.
- Han Cai, Ligeng Zhu, and Song Han. ProxylessNAS: Direct neural architecture search on target task and hardware. In *Proceedings of the 7th International Conference on Learning Representations*, 2019.

- Gari D Clifford, Chengyu Liu, Benjamin Moody, H Lehman Li-wei, Ikaro Silva, Qiao Li, AE Johnson, and Roger G Mark. Af classification from a short single lead ecg recording: The physician/computing in cardiology challenge 2017. In *2017 Computing in Cardiology (CinC)*, pp. 1–4. IEEE, 2017.
- Taco S. Cohen, Mario Geiger, Jonas Koehler, and Max Welling. Spherical CNNs. In *Proceedings of the 6th International Conference on Learning Representations*, 2018.
- ENCODE Project Consortium et al. The encode (encyclopedia of dna elements) project. *Science*, 306(5696):636–640, 2004.
- Ulysse Côté-Allard, Cheikh Latyr Fall, Alexandre Drouin, Alexandre Campeau-Lecours, Clément Gosselin, Kyrre Glette, François Laviolette, and Benoit Gosselin. Deep learning for electromyographic hand gesture signal classification using transfer learning. *IEEE Transactions on Neural Systems and Rehabilitation Engineering*, 27(4):760–771, 2019.
- Angus Dempster, François Petitjean, and Geoffrey I Webb. Rocket: exceptionally fast and accurate time series classification using random convolutional kernels. *Data Mining and Knowledge Discovery*, 34(5):1454–1495, 2020.
- Elizabeth D Dolan and Jorge J Moré. Benchmarking optimization software with performance profiles. *Mathematical programming*, 91(2):201–213, 2002.
- Xuanyi Dong and Yi Yang. NAS-Bench-201: Extending the scope of reproducible neural architecture search. In *Proceedings of the 8th International Conference on Learning Representations*, 2020.
- Yawen Duan, Xin Chen, Hang Xu, Zewei Chen, Xiaodan Liang, Tong Zhang, and Zhenguo Li. TransNAS-Bench-101: Improving transferability and generalizability of cross-task neural architecture search. In *Proceedings of the IEEE Conference on Computer Vision and Pattern Recognition*, 2021.
- Thomas Elsken, Jan Hendrik Metzen, and Frank Hutter. Neural architecture search: A survey. *Journal of Machine Learning Research*, 20(55):1–21, 2019.
- Jiemin Fang, Yuzhu Sun, Qian Zhang, Yuan Li, Wenyu Liu, and Xinggang Wang. Densely connected search space for more flexible neural architecture search. In *Proceedings of the IEEE Conference on Computer Vision and Pattern Recognition*, 2020.
- Eduardo Fonseca, Jordi Pons Puig, Xavier Favory, Frederic Font Corbera, Dmitry Bogdanov, Andres Ferraro, Sergio Oramas, Alastair Porter, and Xavier Serra. Freesound datasets: a platform for the creation of open audio datasets. In *Hu X, Cunningham SJ, Turnbull D, Duan Z, editors. Proceedings of the 18th ISMIR Conference; 2017 oct 23-27; Suzhou, China.[Canada]: International Society for Music Information Retrieval; 2017. p. 486-93. International Society for Music Information Retrieval (ISMIR)*, 2017.
- Eduardo Fonseca, Xavier Favory, Jordi Pons, Frederic Font, and Xavier Serra. Fsd50k: an open dataset of human-labeled sound events. *arXiv preprint arXiv:2010.00475*, 2020.
- John S Garofolo. Timit acoustic phonetic continuous speech corpus. *Linguistic Data Consortium*, 1993, 1993.
- Jort F Gemmeke, Daniel PW Ellis, Dylan Freedman, Aren Jansen, Wade Lawrence, R Channing Moore, Manoj Plakal, and Marvin Ritter. Audio set: An ontology and human-labeled dataset for audio events. In *2017 IEEE International Conference on Acoustics, Speech and Signal Processing (ICASSP)*, pp. 776–780. IEEE, 2017.
- Kaiming He, Xiangyu Zhang, Shaoqing Ren, and Jian Sun. Deep residual learning for image recognition. In *Proceedings of the IEEE Conference on Computer Vision and Pattern Recognition*, 2016.
- Shenda Hong, Yanbo Xu, Alind Khare, Satria Priambada, Kevin Maher, Alaa Aljiffry, Jimeng Sun, and Alexey Tumanov. Holmes: health online model ensemble serving for deep learning models in intensive care units. In *Proceedings of the 26th ACM SIGKDD International Conference on Knowledge Discovery & Data Mining*, pp. 1614–1624, 2020.

- Gao Huang, Zhuang Liu, Laurens Van Der Maaten, and Kilian Q Weinberger. Densely connected convolutional networks. In *Proceedings of the IEEE conference on computer vision and pattern recognition*, pp. 4700–4708, 2017.
- David Josephs, Carson Drake, Andy Heroy, and John Santerre. semg gesture recognition with a simple model of attention. In *Machine Learning for Health*, pp. 126–138. PMLR, 2020.
- John Jumper, Richard Evans, Alexander Pritzel, Tim Green, Michael Figurnov, Kathryn Tunyasuvunakool, Olaf Ronneberger, Russ Bates, Augustin Žídek, Alex Bridgland, Clemens Meyer, Simon A A Kohl, Anna Potapenko, Andrew J Ballard, Andrew Cowie, Bernardino Romera-Paredes, Stanislav Nikolov, Rishub Jain, Jonas Adler, Trevor Back, Stig Petersen, David Reiman, Martin Steinegger, Michalina Pacholska, David Silver, Oriol Vinyals, Andrew W Senior, Koray Kavukcuoglu, Pushmeet Kohli, and Demis Hassabis. High accuracy protein structure prediction using deep learning. In *Fourteenth Critical Assessment of Techniques for Protein Structure Prediction (Abstract Book)*, 2020. URL [https://predictioncenter.org/casp14/doc/CASP14\\_Abstracts.pdf](https://predictioncenter.org/casp14/doc/CASP14_Abstracts.pdf).
- Nikita Klyuchnikov, Ilya Trofimov, Ekaterina Artemova, Mikhail Salnikov, Maxim Fedorov, and Evgeny Burnaev. NAS-Bench-NLP: Neural architecture search benchmark for natural language processing. arXiv, 2020.
- Alex Krizhevksy. Learning multiple layers of features from tiny images. Technical report, 2009.
- Liam Li, Kevin Jamieson, Afshin Rostamizadeh, Ekaterina Gonina, Moritz Hardt, Benjamin Recht, and Ameet Talwalkar. A system for massively parallel hyperparameter tuning. *arXiv preprint arXiv:1810.05934*, 2018.
- Liam Li, Mikhail Khodak, Maria-Florina Balcan, and Ameet Talwalkar. Geometry-aware gradient algorithms for neural architecture search. In *Proceedings of the 9th International Conference on Learning Representations*, 2021a.
- Lisha Li, Kevin G Jamieson, Giulia DeSalvo, Afshin Rostamizadeh, and Ameet Talwalkar. Hyperband: Bandit-based configuration evaluation for hyperparameter optimization. In *ICLR (Poster)*, 2017.
- Zongyi Li, Nikola Borislavov Kovachki, Kamyar Azizzadenesheli, Burigede Liu, Kaushik Bhattacharya, Andrew Stuart, and Anima Anandkumar. Fourier neural operator for parametric partial differential equations. In *Proceedings of the 9th International Conference on Learning Representations*, 2021b.
- Chenxi Liu, Liang-Chieh Chen, Florian Schroff, Hartwig Adam, Wei Hua, Alan L Yuille, and Li Fei-Fei. Auto-deeplab: Hierarchical neural architecture search for semantic image segmentation. In *Proceedings of the IEEE/CVF Conference on Computer Vision and Pattern Recognition*, pp. 82–92, 2019a.
- Hanxiao Liu, Karen Simonyan, and Yiming Yang. DARTS: Differentiable architecture search. In *Proceedings of the 7th International Conference on Learning Representations*, 2019b.
- Abhinav Mehrotra, Alberto Gil, C. P. Ramos, Sourav Bhattacharya, Łukasz Dudziak, Ravichander Vipperla, Thomas Chau, Samin Ishtiaq, Mohamed S. Abdelfattah, and Nicholas D. Lane. NAS-Bench-ASR: Reproducible neural architecture search for speech recognition. In *Proceedings of the 8th International Conference on Learning Representations*, 2021.
- François Petitjean, Jordi Inglada, and Pierre Gançarski. Satellite image time series analysis under time warping. *IEEE transactions on geoscience and remote sensing*, 50(8):3081–3095, 2012.
- Hieu Pham, Melody Y. Guan, Barret Zoph, Quoc V. Le, and Jeff Dean. Efficient neural architecture search via parameter sharing. In *Proceedings of the 35th International Conference on Machine Learning*, 2018.
- Esteban Real, Chen Liang, David R. So, and Quoc V. Le. AutoML-Zero: Evolving machine learning algorithms from scratch. In *Proceedings of the 37th International Conference on Machine Learning*, 2020.

- Nicholas Roberts, Mikhail Khodak, Tri Dao, Liam Li, Chris Ré, and Ameet Talwalkar. Rethinking neural operations for diverse tasks. arXiv, 2021.
- Eleni Triantafillou, Tyler Zhu, Vincent Dumoulin, Pascal Lamblin, Utku Evci, Kelvin Xu, Ross Goroshin, Carles Gelada, Kevin Swersky, Pierre-Antoine Manzagol, and Hugo Larochelle. Meta-dataset: A dataset of datasets for learning to learn from few examples. In *Proceedings of the 8th International Conference on Learning Representations*, 2020.
- Colin White, Willie Neiswanger, and Yash Savani. BANANAS: Bayesian optimization with neural architectures for neural architecture search. In *Proceedings of the 35th AAAI Conference on Artificial Intelligence*, 2021.
- Yuhui Xu, Lingxi Xie, Xiaopeng Zhang, Xin Chen, Guo-Jun Qi, Qi Tian, and Hongkai Xiong. PC-DARTS: Partial channel connections for memory-efficient architecture search. In *Proceedings of the 8th International Conference on Learning Representations*, 2020.
- Chris Ying, Aaron Klein, Eric Christiansen, Esteban Real, Kevin Murphy, and Frank Hutter. NAS-Bench-101: Towards reproducible neural architecture search. In *Proceedings of the 36th International Conference on Machine Learning*, 2019.
- Sergey Zagoruyko and Nikos Komodakis. Wide residual networks. In *Proceedings of the British Machine Vision Conference*, 2016.
- Arber Zela, Julien Siems, and Frank Hutter. NAS-Bench-1Shot1: Benchmarking and dissecting one-shot neural architecture search. In *Proceedings of the 8th International Conference on Learning Representations*, 2020.
- Keming Zhang and Joshua S Bloom. deeper: Cosmic ray rejection with deep learning. *The Astrophysical Journal*, 889(1):24, 2020.
- Zijun Zhang, Evan M Cofer, and Olga G Troyanskaya. Ambient: accelerated convolutional neural network architecture search for regulatory genomics. *bioRxiv*, 2021a.
- Zijun Zhang, Christopher Y Park, Chandra L Theesfeld, and Olga G Troyanskaya. An automated framework for efficiently designing deep convolutional neural networks in genomics. *Nature Machine Intelligence*, 3(5):392–400, 2021b.
- Jian Zhou and Olga G Troyanskaya. Predicting effects of noncoding variants with deep learning-based sequence model. *Nature methods*, 12(10):931–934, 2015.
- Barret Zoph, Vijay Vasudevan, Jonathon Shlens, and Quoc V. Le. Learning transferable architectures for scalable image recognition. In *Proceedings of the IEEE Conference on Computer Vision and Pattern Recognition*, 2018.

## A Comparison of NAS with Expert Architectures

We create a more challenging baseline for NAS by evaluating hand-designed architectures for each specific task. Hand-crafted networks are selected according to best-effort search. The full evaluation results of NAS methods vs. non-NAS baselines can be found in Table 5. Figure 4 illustrates a comparison between best-performing NAS methods vs. best non-NAS methods. Surprisingly, GAEA PC-DARTS beats all the baselines on a portion of the tasks.

Here is a brief summary of these expert models and their citations:

1. DenseNet-BC (CIFAR-100): a more sophisticated version of ResNet, achieving state-of-the-art performance on vision classification (Huang et al., 2017).
2. S2CNN (Spherical): a spherical CNN contains special operations designed for spherical signals, state-of-the-art on spherically-projected MNIST (Cohen et al., 2018).
3. Fourier Neural Operator (FNO) Network (Darcy Flow): via parametrization in Fourier space, FNO can efficiently learn a family of partial differential equations and their mapping to solutions (Li et al., 2021b).
4. DEEPCON (PSICOV): a dilated-convolution neural network combined with dropout to optimize for protein distance prediction (Adhikari, 2020a).
5. deepCR-mask (Cosmic): a modified version of UNet retaining data dimension to keep pixels at the borders to suit astronomy applications, state-of-the-art on this task (Zhang & Bloom, 2020).
6. Attention-based model (NinaPro): a lightweight feed-forward neural network adopting attention modules in place of convolutions (Josephs et al., 2020).
7. VGG-like (FSD50K): a smaller VGG network with output features combining both global max pooling and average pooling for audio (Fonseca et al., 2020).
8. ResNet-1D (ECG): ResNet with 1D convolution, using a larger kernel size of 16 and a stride of 2 for all convolutions. The architecture is state-of-the-art on several time-series prediction tasks in medicine (Hong et al., 2020).
9. ROCKET (Satellite): a simple linear classifier with random convolution kernel as a feature extractor, achieving state-of-the-art performance on UCR time-series prediction tasks (Dempster et al., 2020).
10. DeepSEA model (DeepSEA): the original 1D convolution model accompanying the dataset, state-of-the-art on DeepSEA itself (Zhou & Troyanskaya, 2015).

## B Experiment Details

### B.1 Hyperparameter Tuning and Backbone

We use a wide residual network with 16 layers and a widening factor of 4 (WRN-16-4) for all tasks.

For tuning hyperparameters, we use ASHA’s default elimination schedule and search over 7 to 256 randomly sampled hyperparameter configurations matching GAEA PC-DART’s runtime. The maximum epochs that a single configuration could be trained is equal to that of Wide ResNet’s default, 200.

We have selected the following hyperparameter ranges for tuning the Wide ResNet backbone:

- $\log_{10}$ (learning rate): Unif[-4, -1]
- momentum: Unif{0.0, 0.3, 0.6, 0.9}
- $\log_{10}$ (weight decay): Unif[-5, -2]
- dropout: Unif{0.0, 0.3, 0.6}
- batch size: 128 (all point tasks except FSD50K), 4 (Darcy Flow), 8 (PSICOV, Cosmic), 256(FSD50K, ECG, Deepsea), 4096 (Satellite)

Table 4: Experiment training runtimes of NAS-Bench-360 (GPU hours)

Task	GAEA	DenseNAS	WRN	AMBER / Auto-DeepLab
CIFAR-100	9.5	2.5	2	n/a
Spherical	16.5	2.5	2	n/a
Darcy Flow	6.5	0.5	0.5	5.5
PSICOV	18	24	18.5	19
Cosmic	21.5	2.5	4	17.5
NinaPro	0.5	0.2	0.2	n/a
FSD50K	37	4.5	4	n/a
ECG	140	6.5	5	27
Satellite	28	3	4.5	26
DeepSEA	39.5	2	1.5	28

## B.2 Reference Runtimes

Using a Nvidia V100 GPU, we have recorded the following runtimes for each experiment in this benchmark in Table 4. Overall, GAEA PC-DARTS is more costly than backbone with hyperparameter optimization, which is more costly than DenseNAS. The protein tasks requires heavy computation since the data is not static but generated during training.

## B.3 Model sizes and FLOPS statistics

As part of the experiment statistics summary, full information of model parameter counts and FLOPs can be found in Table 6 and Table 7. The searched architecture statistics are taken from three random seeds, whereas the fixed models do not vary in size and FLOPS.

## B.4 Adjustments for Dense Prediction Tasks

On the wide ResNet backbone, we add an adaptive averaging pooling operation to upsample the features back to their original dimensions before output. On the DARTS space, we prevent downsampling and keep spatial dimensions unchanged by disabling reduction cells and replacing them with normal cells. On DenseNAS, we configure the super-network to contain only blocks with the original spatial dimensions.

## B.5 Adjustments for 1D Prediction Tasks

The WRN-1D does not have a convolution stem and uses larger kernel sizes of 8,5,3 in each convolution block. We substitute 2D operations with 1D operations within the DARTS and DenseNAS search spaces.

## B.6 Random Seeds

For main experiments, we fix the random seed to be 0,1,2 for each of the 3 trials respectively.

For AMBER experiments, we completed three trials as the package did not offer the option of setting random seeds.

## B.7 Correlation between Performance and Model Size

We plot performances of 30 random architectures from the DenseNAS search space across three tasks in Figure 3. From our random search experiment, larger models searched by NAS are not always better-performing. We study the Pearson correlation coefficient between test performance vs. model size in number of parameters for three tasks: FSD50K, Cosmic, and ECG. On Cosmic and ECG, the

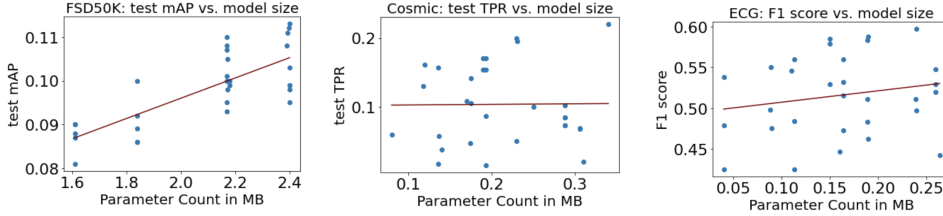


Figure 3: Performances v. Model sizes for three sample tasks.

correlation is very weak ( $r = 0.01$  and  $r = 0.19$  respectively). On FSD50K, a stronger correlation ( $r = 0.79$ ) is observed but performance varies significantly even for architectures of the same size.

## C Supplementary Materials

### C.1 Code and Datasets

Our code is available on GitHub: <https://github.com/rtu715/NAS-Bench-360>

The datasets, along with their documentation, metadata, etc., can be viewed and downloaded on GitHub pages: <https://nb360.ml.cmu.edu/>

### C.2 Data License

- CIFAR-100: CC BY 4.0 (on <https://www.tensorflow.org/datasets/catalog/cifar100>)
- Spherical CIFAR-100: CC BY-SA
- NinaPro: CC BY-ND
- FSD50k: CC BY 4.0
- Darcy Flow: MIT
- DeepCov, PSICOV: GPL
- Cosmic: Open License (<https://registry.opendata.aws/hst/>)
- ECG: ODC-BY 1.0
- Satellite: GPL 3.0
- Deepsea: CC BY 4.0

### C.3 Data Preprocessing Details

**CIFAR-100:** while the 10,000 testing images are kept aside only for evaluating architectures, the 50,000 training images are randomly partitioned into 40,000 for architecture search and 10,000 for validation. On all of the 50,000 training images, we apply standard CIFAR augmentations including random crops and horizontal flipping, and finally normalize them using a pre-calculated mean and standard deviation of this set. On the 10,000 testing images, we only apply normalization with the same constants.

**Spherical:** with the same split ratios CIFAR-100, the generated spherical image data is directly used for training and evaluation without data augmentation and pre-processing.

**NinaPro:** Containing less than 4,000 samples, the data is comprised of single-channel signals with an irregular shape of  $16 \times 52$  pixels. This task also differs from CIFAR for its class imbalance, as over 65% of all gestures are the neutral position. We split the data using the same ratio as CIFAR, resulting in 2638 samples for training, and 659 samples for validation and testing each. No additional pre-processing is performed.



**FSD50K:** The raw sound files are first resampled at a frequency of 22,050 Hz and transformed into 96-band, log-mel spectrograms, which is a representation of the sound’s power spectrum. Small overlapping audio chunks of 1 second are obtained from these larger clips, resulting in an input size of 101\*96 (101 frames of 96-band spectrograms). As data augmentation, background noise of the same frequency is also mixed into 75% of the training data. We split 4,170 clips into the validation set and 10,231 clips into the test set following the original paper. During training, we train on one randomly-sampled chunk, instead of all chunks, from each clip.

**Darcy Flow:** we use scripts provided by (Li et al., 2021b) to generate the PDEs and their solutions, for a total of 900 data points for training, 100 for validation, and 100 for testing. All input data is normalized with constants calculated on the training set before fed into the neural network and de-normalized following an encode-decode scheme. The solutions, or labels, for the training set are also encoded and decoded this way. The test labels are not processed.

**PSICOV:** we adopt the chosen subset of DeepCov proteins in (Adhikari, 2020b), consisting of 3,456 proteins each with 128\*128 feature maps across 57 channels. 100 proteins from this set are used for validation and the rest for training. Test data for final evaluation is gathered from another set of 150 proteins, PSICOV. Since these produce feature maps that are larger (512\*512), we run the prediction network over all of its non-overlapping 128\*128 patches.

**Cosmic:** we use data from a specific filter, F435W, of the space telescope, representing the 3605–4882 Å spectral range. Image stamps of 256\*256 pixels are taken from large images. The dataset contains 4,347 stamps for training, and 420 for test, and 483 for validation to match the test set size.

**ECG:** from the sliding window approach, 12,186 single lead recordings are converted into more than 330,000 recording segments comprised of 261,740 for training, 33,281 for validation, and 33,494 for test. Each segment is of the shape 1\*1,000, representing one channel of 1,000-long temporal sequence.

**Satellite:** each satellite time-series is single-channel of length 46 (1\*46). After applying standard normalization, we divide the one million entries to 800,000 for training, 100,000 for validation, and 100,000 for test. Zero-padding to 48-length sequences is required for DenseNAS’ downsampling network.

**DeepSEA:** the genome sequences are 1,000-base pair (bp) long and represented as a 1000\*4 binary matrix, as each bp is represented as an one-hot encoding corresponding to either A,C,T,G at that location. Total training set size is 71,753. Validation and test sizes that are not subsampled are 2,490 and 149,400 respectively.

Table 5: Performance of NAS vs. non-NAS baselines across the tasks of NAS-Bench-360. All results are averages of three random seeds.

Search space	Search algorithm	CIFAR-100 0-1 error <sup>l</sup>	Spherical 0-1 error <sup>l</sup>	Darcy Flow relative $\ell_2$ <sup>l</sup>	PSICOV MAE <sub>8</sub> <sup>l</sup>	Cosmic FNR <sup>l</sup>
DenseNAS	random	25.49±0.41	71.23±1.65	0.071±0.006	3.70±0.06	70.42±6.07
DenseNAS	original	25.98±0.38	72.99±0.95	0.10±0.01	3.84±0.15	79.52±2.20
DARTS	GAEA	24.02±1.92	<b>48.23±2.87</b>	0.026±0.001	<b>2.94±0.13</b>	31.15±3.48
Auto-DL	DARTS	n/a	n/a	0.049±0.005	6.73±0.73	99.79±0.02
WRN	default	23.35±0.05	85.77±0.71	0.073±0.001	3.84±0.053	51.76±2.09
WRN	ASHA	23.39±0.01	75.46±0.40	0.066±0.00	3.84±0.05	37.53±10.16
Expert	default	<b>19.39±0.20</b>	67.41±0.76	<b>0.008±0.001</b>	3.35±0.14	<b>25.29±1.44</b>

Search space	Search algorithm	NinaPro 0-1 error <sup>l</sup>	FSD50K mAP <sup>h</sup>	ECG F1 score <sup>h</sup>	Satellite 0-1 error <sup>l</sup>	DeepSEA AUROC <sup>h</sup>
DenseNAS	random	8.45±0.56	<b>0.40±0.001</b>	0.58±0.01	13.91±0.13	0.60±0.001
DenseNAS	original	10.17±1.31	0.36±0.002	0.60±0.01	13.81±0.69	0.60±0.001
DARTS	GAEA	17.67±1.39	0.06±0.02	0.66±0.01	<b>12.51±0.24</b>	0.64±0.02
AMBER	ENAS	n/a	n/a	0.67±0.015	12.97±0.07	0.68±0.01
WRN	default	<b>6.78±0.26</b>	0.08±0.001	0.57±0.01	15.49±0.03	0.60±0.001
WRN	ASHA	7.34±0.76	0.09±0.03	0.57±0.01	15.84±0.52	0.59±0.002
Expert	default	8.73±0.90	0.38±0.004	<b>0.72±0.00</b>	19.80±0.00	<b>0.70±0.024</b>

<sup>h/l</sup> a higher / lower value of the metric indicates better performance.

Table 6: Parameter counts of searched and baseline models for all tasks of NAS-Bench-360. Searched model sizes are reported as mean±standard deviation of three random seeds. Results are reported in millions (M). Architectures with the best performance are bolded.

Search space	Search algorithm	CIFAR-100	Spherical	Darcy Flow	PSICOV	Cosmic
DenseNAS	random	1.74±0.12	2.23±0.47	1.00±0.18	1.21±0.16	0.25±0.06
DenseNAS	original	2.03±0.53	1.84±0.15	0.38±0.13	0.93±0.36	0.15±0.16
DARTS	GAEA	4.92±0.28	<b>1.67±0.14</b>	0.63±0.08	<b>0.53±0.05</b>	0.43±0.15
Auto-DL	DARTS	n/a	n/a	22.98±3.49	6.50±1.84	7.61±2.14
WRN	default	2.77	2.77	2.75	2.76	2.75
Expert	default	<b>3.08</b>	0.16	<b>1.19</b>	0.60	<b>0.10</b>

Search space	Search algorithm	NinaPro	FSD50K	ECG	Satellite	DeepSEA
DenseNAS	random	6.80±0.46	<b>2.40±0.00</b>	0.18±0.05	0.79±0.16	0.25±0.04
DenseNAS	original	6.69±0.53	1.45±0.00	0.11±0.05	1.08±0.63	0.19±0.00
DARTS	GAEA	3.35±0.48	0.81±0.11	3.31±0.07	<b>3.35±0.35</b>	2.91±0.47
AMBER	ENAS	n/a	n/a	6.61±0.33	6.22±1.36	8.44±1.47
WRN	default	<b>2.75</b>	2.80	0.50	0.51	0.51
Expert	default	1.36	0.35	<b>16.5</b>	0.48	<b>60.9</b>

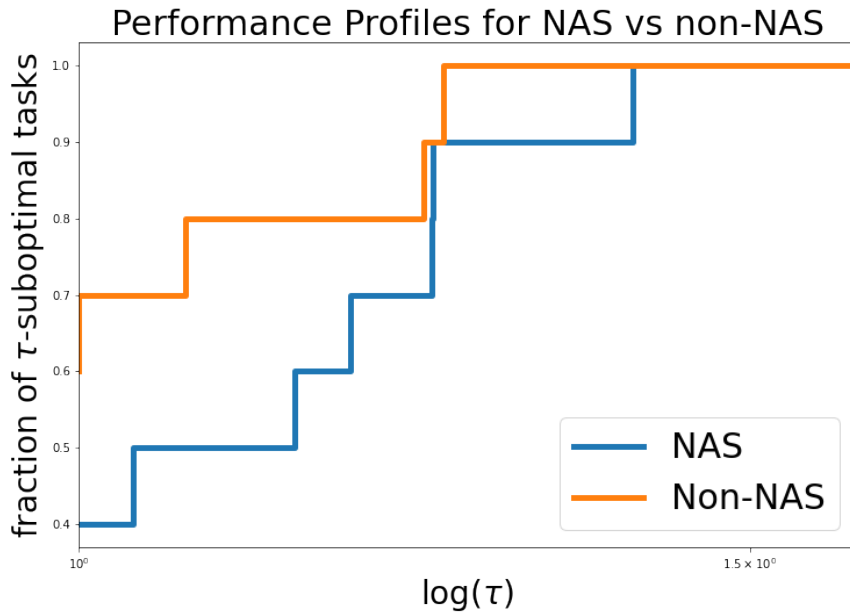


Figure 4: Performance profiles on all tasks for best-performing NAS vs. Non-NAS. A larger value indicates a larger fraction of tasks on which the method is within a multiplicative factor  $\tau$  of the best method.

Table 7: FLOPS of searched and baseline models for all tasks of NAS-Bench-360. Searched model FLOPS are reported as mean $\pm$ standard deviation of three random seeds. Results are reported in GFLOPS. Architectures with the best performance are bolded.

Search space	Search algorithm	CIFAR-100	Spherical	Darcy Flow	PSICOV	Cosmic
DenseNAS	random	0.46 $\pm$ 0.07	0.91 $\pm$ 0.07	14.42 $\pm$ 2.58	39.80 $\pm$ 5.09	8.42 $\pm$ 2.11
DenseNAS	original	0.44 $\pm$ 0.53	1.84 $\pm$ 0.15	5.43 $\pm$ 1.82	30.51 $\pm$ 11.90	5.00 $\pm$ 5.30
DARTS	GAEA	1.42 $\pm$ 0.09	<b>1.91<math>\pm</math>0.65</b>	9.33 $\pm$ 1.13	<b>17.74<math>\pm</math>1.68</b>	14.27 $\pm$ 4.90
Auto-DL	DARTS	n/a	n/a	2.54 $\pm$ 1.20	3.43 $\pm$ 1.27	2.44 $\pm$ 0.26
WRN	default	0.78	2.78	39.72	90.58	90.06
Expert	default	<b>1.18</b>	n/a	<b>n/a</b>	0.01	<b>1.96</b>
Search space	Search algorithm	NinaPro	FSD50K	ECG	Satellite	DeepSEA
DenseNAS	random	1.02 $\pm$ 0.06	<b>0.40<math>\pm</math>0.00</b>	0.11 $\pm$ 0.02	0.02 $\pm$ 0.01	0.15 $\pm$ 0.02
DenseNAS	original	0.97 $\pm$ 0.14	0.80 $\pm$ 0.00	0.16 $\pm$ 0.03	0.02 $\pm$ 0.01	0.10 $\pm$ 0.00
DARTS	GAEA	0.89 $\pm$ 0.12	2.57 $\pm$ 0.47	2.28 $\pm$ 0.05	<b>0.11<math>\pm</math>0.07</b>	2.01 $\pm$ 0.33
AMBER	ENAS	n/a	n/a	0.03 $\pm$ 0.01	0.03 $\pm$ 0.01	0.04 $\pm$ 0.01
WRN	default	<b>0.64</b>	7.56	1.02	0.04	1.02
Expert	default	0.02	0.66	<b>0.70</b>	0.01	<b>0.12</b>

\*some expert models contain non-standard modules without FLOPS count.